XXI IMEKO World Congress "Measurement in Research and Industry"
August 30 – September 4, 2015, Prague, Czech Republic

INTERPOLATION IN A DIGITAL UNBALANCED IMPEDANCE COMPARATOR

Kamil Kontorski

University of Zielona Góra, Department of Electrical Engineering, Computer Science and Telecommunication, Institute of Electrical Metrology, Zielona Góra, Poland, k.kontorski@ime.uz.zgora.pl

Abstract – Some details about digital balanced and unbalanced impedance comparators are presented in this article. A method of measuring an impedance ratio using the digital unbalanced comparator is described. Considerations about measurement errors connected with an experimental comparator setup are included. The research results are in an agreement with the theoretical assumptions.

Keywords: balanced and unbalanced digital impedance comparator, interpolation, DFT, digital acquisition card, DAQ

1. INTRODUCTION

Over forty years ago measurement systems started employing voltage generators which construction is based on Direct Digital Synthesis. The sources based on this technique are often called DSS (Digital Sinewave Sources). Impedance comparators based on calibrated [1, 2] and non-calibrated [3] sources appear in the area of precise electrical measurements. The electrical diagrams of typical comparators with two DSS are presented in Fig. 1.

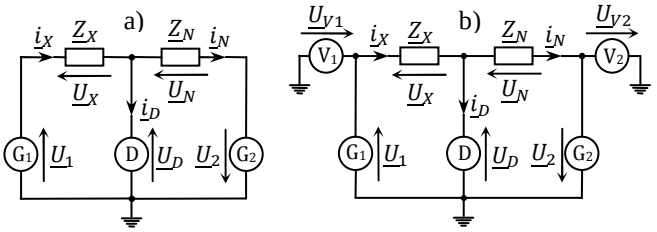

Fig. 1. Electrical diagrams of the comparators with two DSS: a) with calibrated sources, b) with non-calibrated sources.

The bridge in Fig. 1a is brought into a balance state by setting the appropriate values of the amplitudes and phases of the two DSS marked as G_1, G_2. This state is established when detector D indicates the zero voltage value ($\underline{U}_D = 0$) across the measurement diagonal. The ratio of impedances $\underline{Z}_X$, $\underline{Z}_N$ is derived from the settings values $\underline{U}_1$, $\underline{U}_2$ of the two DSS. The settings ratio is represented by variable $\underline{K}_U$. In the fig. 1b a diagram of the comparator is shown which functions in the analogous manner like the comparator in fig. 1a. But when the bridge in the fig. 1b is balanced the DSS settings are measured by voltmeters V_1, V_2. The settings ratio $\underline{U}_{Y1}/\underline{U}_{Y2}$ is now represented by variable $\underline{K}_{UV}$. The voltages are represented by the complex values of the fundamental harmonics of measured periodic signals.

The balanced comparator is able to work as an unbalanced comparator. The equation describing the bridge presented in the Fig. 1b has the following form

$$\underline{K}_Z - \underline{K}_{UV} = \underline{U}_{D,r}\underline{k}_r, \tag{1}$$

where:

$$\underline{K}_Z = \underline{Z}_X/\underline{Z}_N,\ \underline{K}_{UV} = \underline{U}_{Y1}/\underline{U}_{Y2},\ \underline{U}_{D,r} = \underline{U}_D/\underline{U}_{Y2},$$
$$\underline{k}_r = -\left(1 + \underline{K}_Z\underline{K}_P\right),\ \underline{K}_P = 1 + \underline{Z}_N/\underline{Z}_D.$$

Variable $\underline{Z}_D$ represents all impedances through which a current flows from the bridge diagonal to the ground. Its value depends on connecting coaxial cables impedances, $\underline{Z}_X$ and $\underline{Z}_N$ ground impedances and a detector impedance.

Studies related to the digital unbalanced comparator are presented in work [6]. Results of experimental researches achieved by the balanced and unbalanced bridge are in an agreement with theoretical assumptions. But, to determine the impedance ratio it is required to know the values of $\underline{Z}_D$ and $\underline{Z}_N$ impedances which is time-consuming.

In this article an idea of measuring the impedance ratio using the unbalanced comparator is presented. It does not require additional measurements of $\underline{Z}_D$ and $\underline{Z}_N$.

2. INTERPOLATION METHOD

2.1. Equations of the measurement method

The interpolation method uses two different settings ratios $\underline{K}'_U$, $\underline{K}''_U$. Its measured values are marked as $\underline{K}'_{UV}$, $\underline{K}''_{UV}$. Two relative unbalance voltages corresponding to that settings are designated by $\underline{U}'_{D,r}$, $\underline{U}''_{D,r}$. We can write the following system of two equations:

$$\underline{k}_r\underline{U}'_{D,r} = \underline{K}_Z - \underline{K}'_{UV}, \tag{2}$$

$$\underline{k}_r\underline{U}''_{D,r} = \underline{K}_Z - \underline{K}''_{UV}. \tag{3}$$

Using the above equations we can present the impedance ratio in the following form

$$\underline{K}_Z = \frac{\underline{U}''_{D,r}\underline{K}'_{UV} - \underline{U}'_{D,r}\underline{K}''_{UV}}{\underline{U}''_{D,r} - \underline{U}'_{D,r}}. \tag{4}$$

The above formula does not involve the parasitic impedance $\underline{Z}_D$ nor the standard impedance $\underline{Z}_N$. Inconvenience connected with (4) is its complicated form.

The way in which the values of $\underline{K}_U'$ and $\underline{K}_U''$ are determined is the regard which need to be analysed.

2.2. Determination of the DSS settings

The values of the settings will be chosen to preserve that the modulus of the current flowing through $\underline{Z}_X$ is the same for both settings. The same treatment is applied for the current flowing through $\underline{Z}_D$. This approach is especially efficient when the values of the impedances depend on the voltages values applied to them. The set of equations that describe the above conditions are shown below:

$$\left|\underline{U}_{D,r}'\right| = \left|\underline{U}_{D,r}''\right|,$$
$$\left|\underline{K}_U' - \underline{U}_{D,r}'\right| = \left|\underline{K}_U'' - \underline{U}_{D,r}''\right|.$$

Using the designations applied in (1) the above equations can be modified into the following form:

$$\left|\underline{K}_U' - \underline{K}_Z\right| = \left|\underline{K}_U'' - \underline{K}_Z\right|, \tag{5}$$
$$\left|\underline{K}_U' + \frac{1}{\underline{K}_P}\right| = \left|\underline{K}_U'' + \frac{1}{\underline{K}_P}\right|. \tag{6}$$

A graph presented in Fig. 2 is helpful in solving the set of equations (5-6). The center, O, of the bigger circle has a coordinates equal to $-1/\underline{K}_P$ and the radius equal to the modulus, $\left|1/\underline{K}_P + \underline{K}_Z\right|$. The center, P, of the second circle has the coordinates equal to $\underline{K}_Z$. The points where the two circles cross determine the values which corresponds to requested settings $\underline{K}_U'$ and $\underline{K}_U''$.

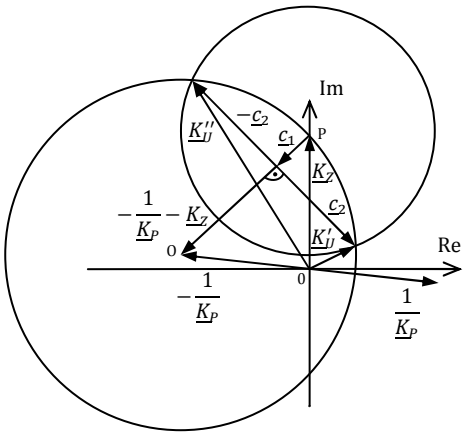

Fig. 2. An exemplar graph that is helpful in solving the set of equations (5-6).

The solutions of (5-6) are presented below:

$$\underline{K}_U' = \underline{K}_Z + \underline{c}_1 + \underline{c}_2, \tag{7}$$
$$\underline{K}_U'' = \underline{K}_Z + \underline{c}_1 - \underline{c}_2. \tag{8}$$

The vectors corresponding to variables $\underline{c}_1$ and $\underline{c}_2$ are shown in Fig. 2. The expressions describing them are shown below:

$$\underline{c}_1 = -k_i\left(\frac{1}{\underline{K}_P} + \underline{K}_Z\right), \tag{9}$$

$$\underline{c}_2 = \mathrm{j}\underline{c}_1\sqrt{\left(\frac{2}{k_i} - 1\right)}. \tag{10}$$

where k_i is a real number from the range $\langle 0,2\rangle$.

3. MEASUREMENT ERRORS

The variables described by (2-3) will be presented in the following form:

$$\underline{K}_{UV}' = \frac{\underline{U}_{11}}{\underline{U}_{21}}, \underline{K}_{UV}'' = \frac{\underline{U}_{12}}{\underline{U}_{22}}, \underline{U}_{D,r}' = \frac{\underline{U}_{D1}}{\underline{U}_{21}}, \underline{U}_{D,r}'' = \frac{\underline{U}_{D2}}{\underline{U}_{22}}.$$

Triples of voltages $\underline{U}_{11}$, $\underline{U}_{21}$, $\underline{U}_{D1}$ and $\underline{U}_{12}$, $\underline{U}_{22}$, $\underline{U}_{D2}$ correspond to the triple of voltages $\underline{U}_{y1}$, $\underline{U}_{y2}$, $\underline{U}_D$ shown on Fig. 1b. Now, the impedance ratio can be expressed in the following form

$$\underline{K}_Z = \frac{\underline{U}_{D2}\underline{U}_{11} - \underline{U}_{D1}\underline{U}_{12}}{\underline{U}_{D2}\underline{U}_{21} - \underline{U}_{D1}\underline{U}_{22}}. \tag{11}$$

3.1. Errors caused by a multiplexer

A multiplexer is shown in Fig. 5 which presents the experimental setup. The detailed electrical diagram of the multiplexer is shown in Fig. 3. Variable R_{on} represents the resistance of the multiplexer channels when they are in on state. Variable C_{off} represents the capacitances of the channels when they are in off state. The input channels of the multiplexer are designated by chan_1, chan_2, chan_3.

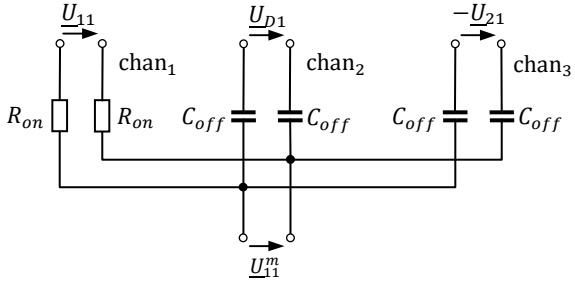

Fig. 3. An electrical diagram of the multiplexer.

The voltages $\underline{U}_{11}^m$, $\underline{U}_{D1}^m$, $\underline{U}_{21}^m$ at the output of the multiplexer correspond to the voltages $\underline{U}_{11}$, $\underline{U}_{D1}$, $-\underline{U}_{21}$ at the input. If we assume that one terminal of each measured voltage is on the same relatively low potential then the relations between the voltages can be presented in the following way:

$$\underline{U}_{11} \approx \underline{U}_{11}^m - \underline{k}_m\left(\underline{U}_{D1}^m + \underline{U}_{21}^m\right), \tag{12}$$
$$\underline{U}_{D1} \approx \underline{U}_{D1}^m - \underline{k}_m\left(\underline{U}_{11}^m + \underline{U}_{21}^m\right), \tag{13}$$
$$-\underline{U}_{21} \approx \underline{U}_{21}^m - \underline{k}_m\left(\underline{U}_{11}^m + \underline{U}_{D1}^m\right), \tag{14}$$

where:
$\underline{k}_m = \mathrm{j}\omega R_{on} C_{MW}$,
$C_{MW} = C_{W+} + 2C_{off}$,
C_{W+} – input capacitance of the voltmeter.

Analogous relations and designations that appear in (12-14) are applied for the voltages $\underline{U}_{12}$, $\underline{U}_{22}$, $\underline{U}_{D2}$.

It can be proved that a comparison error caused by the multiplexer in the unbalanced comparator that uses the interpolation can be presented in the following form

$$\underline{\Delta}_{K_Z,M} \approx \underline{k}_m\left(\underline{K}_Z - 1\right)\left(\underline{K}_P - 1\right). \tag{15}$$

It can be also proved that (15) describes the error in the balanced comparator.

3.2. Errors caused by a voltmeter

In Fig. 4 a functional diagram of a voltmeter is presented. It employs a successive approximation ADC. The variables C_{W+}, C_{W-} and R_{W+}, R_{W-} represents the values of the input capacitance and resistance respectively between the input terminals, In + and In–, and the ground. The input stage does not affect the fundamental harmonic $\underline{U}_{11}^{m}$ of the input signal. A low-pass anti-alliasing filter has the 40 kHz cut-off frequency. The variable $\underline{k}_{DP}$ represents the filter voltage transmittance. Probes from the ADC are sent to Microprocessor System and Discrete Fourier Transform is used to determine the fundamental harmonic marked as $\underline{U}_{11}^{V}$.

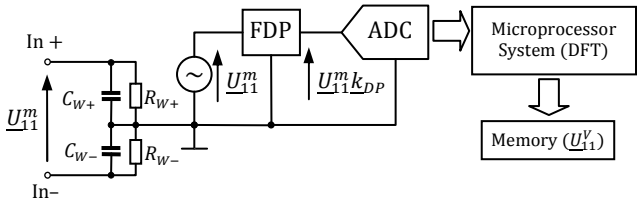

Fig. 4. A functional diagram of the voltmeter.

The output voltages of the multiplexer $\underline{U}_{11}^{m}$, $\underline{U}_{D1}^{m}$, $\underline{U}_{21}^{m}$ are applied on the input of the voltmeter. The voltages corresponding to them at the output are marked as $\underline{U}_{11}^{V}$, $\underline{U}_{D1}^{V}$, $\underline{U}_{21}^{V}$. The relations between these voltages may be presented in the following form:

$$\underline{U}_{11}^{m}\underline{k}_{DP} + \underline{\Delta}_{L}^{\underline{U}_{11}} + \underline{\Delta}_{K}^{\underline{U}_{11}} = \underline{U}_{11}^{V}, \tag{16}$$

$$\underline{U}_{D1}^{m}\underline{k}_{DP} + \underline{\Delta}_{L}^{\underline{U}_{D1}} + \underline{\Delta}_{K}^{\underline{U}_{D1}} = \underline{U}_{D1}^{V}, \tag{17}$$

$$\underline{U}_{21}^{m}\underline{k}_{DP} + \underline{\Delta}_{L}^{\underline{U}_{21}} + \underline{\Delta}_{K}^{\underline{U}_{21}} = \underline{U}_{21}^{V}, \tag{18}$$

where:

$\underline{\Delta}_{L}^{\underline{U}_{11}}$, $\underline{\Delta}_{L}^{\underline{U}_{D1}}$, $\underline{\Delta}_{L}^{\underline{U}_{21}}$ – absolute errors caused by the nonlinearities of the ADC,

$\underline{\Delta}_{K}^{\underline{U}_{11}}$, $\underline{\Delta}_{K}^{\underline{U}_{D1}}$, $\underline{\Delta}_{K}^{\underline{U}_{21}}$ – absolute errors caused by the quantization of the ADC.

Analogous relations and designations that appear in (16-18) apply for the voltages $\underline{U}_{12}^{m}$, $\underline{U}_{22}^{m}$, $\underline{U}_{D2}^{m}$.

When the complex voltage ratio is to be computed then the coefficient $\underline{k}_{DP}$ can be reduced. This is true when the electrical parameters of the experimental system that correspond to this variable are constant in time.

If we assume that there is no relation between values of the quantization errors of particular probes then the errors $\underline{\Delta}_{K}^{\underline{U}_{11}}$, $\underline{\Delta}_{K}^{\underline{U}_{21}}$, $\underline{\Delta}_{K}^{\underline{U}_{D1}}$, $\underline{\Delta}_{K}^{\underline{U}_{12}}$, $\underline{\Delta}_{K}^{\underline{U}_{22}}$, $\underline{\Delta}_{K}^{\underline{U}_{D2}}$ become smaller with larger number of probes acquired [4].

We cannot minimize the errors caused by ADC nonlinearities by acquiring more probes. It will be assumed that this error is proportional to the modulus of the sampled voltage fundamental harmonic and that it has the same value for the real and imaginary part of that fundamental. This error for $\underline{U}_{11}$ voltage may be written in the following form

$$\underline{\Delta}_{L}^{\underline{U}_{11}} = |\underline{U}_{11}|\delta_L + \mathrm{j}|\underline{U}_{11}|\delta_L. \tag{19}$$

where δ_L is the relative linearity limit error of the ADC.

If we assume that $|\underline{U}_{D1}/\underline{U}_{21}|$, $|\underline{U}_{D2}/\underline{U}_{22}|$ < 10 mV/V then it can be proved that the comparison error, $\Delta_{\underline{K}_{Z,L}}$, caused by the ADC nonlinearities takes the following form

$$\underline{\Delta}_{\underline{K}_{Z,L}} \approx |\underline{K}_Z|\delta_L + \mathrm{j}|\underline{K}_Z|\delta_L. \tag{20}$$

It can be proved that linearity error in the balanced comparator is the same as (20) but multiplied by $\sqrt{2}$.

3.3. Errors caused by coaxial cables

The influence of the coaxial cables on the comparison error in the digital balanced and unbalanced comparator is the same. Research results show that errors are negligible if good quality cables are used and if impedances under test have the absolute value above 10 kΩ.

4. EXPERIMENTAL RESULTS

4.1. Experimental setup diagram

An experimental setup electrical diagram is presented in Fig. 5. We can see the multiplexer (MUX), the voltmeter (FDP&ADC), the digital generators (DAC_1, DAC_2).

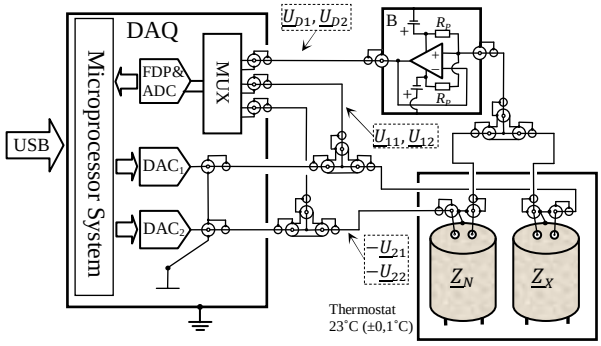

Fig. 5. A diagram of the experimental setup.

These elements are enclosed in the DAQ card USB-6281 from National Instruments. The buffer B includes two polarization resistors R_P which values are equal to 20 MΩ. The impedances under test are placed in the thermostat. All cables in the diagram are 1 m long.

4.2. Configuration of the DAQ card elements

First of two DSS, DAC_1, is responsible for balancing the bridge. Its voltage range is changing according to the values of generated probes. The voltage range of the second DSS, DAC_2, is constant and equal to ±1 V. Both generators have the same time-base source with the frequency equal to 20 MHz. Each probe is generated after 20 cycles. Generators start when the rising edge of the signal generated by a counter occurs. The acquisition of the probes is delayed for 5 seconds to make the voltages more stable. The number of probes generated in one period is changing from 2000 to 96.

The voltmeter inputs are configured to work in differential mode. The time-base of the voltmeter is the same as for the generators. The sampling frequency is equal to 500 kHz. One voltage is sampled for 2 seconds. The way the probes are gathered is described in [5]. The beginning of the sampling is invoked by the signal from a counter. The number of acquired probes is always a multiplication of 4.

Internal counter CTR0 produces digital signal which synchronizes the beginnings of the generations and acquisitions of the signals. The time-base of the counter is the same as for generators and voltmeter.

4.3. Experimental results

Standard resistors used in the experiments have the following values: 10 kΩ, 10 kΩ and 100 kΩ. These are film resistors from Vishay. Each of them is enclosed in a metal can with the 2TP terminals. Their temperature coefficients equal approximately to $0{,}1\times10^{-6}$/°C.

The type of the capacitors used in the experiments is P597. Their rated values are equal to 1 nF, 3 nF, 3 nF and 10 nF. The temperature coefficient is less than 15×10^{-6}/°C. The loss factor is less than 0,0005 for the frequencies below 1 kHz. They have the 3T measurement terminals.

In the case of balanced comparator the following equation is used to determine the impedance ratio

$$\underline{K_Z} = \frac{\underline{U_1}-\underline{U_D}}{\underline{U_2}+\underline{U_D}}. \tag{21}$$

The errors caused by the coaxial cables and multiplexer should be added to the measurement results. But in case of accuracy comparison between two comparators it is not necessary to enlarge the results by the same values. It is assumed that the differences in the results are caused only by the linearity errors expressed by (20).

In Fig. 6-13 the panes represent the results returned by the balanced comparator and the squares represents the results returned by the unbalanced comparator with interpolation for $k_i = 0{,}0001$. This corresponds to unbalance voltage absolute value of about 10 mV/V. The horizontal axis is the frequency. The results acquired by the unbalanced comparator are marked for 100 Hz higher frequency than the results acquired by the balanced comparator to provide a better readability. The vertical axis represents the real or imaginary part of $\underline{K_Z}$. The error bars are derived from (20) for δ_L equal to 10×10^{-6}. Each point is a three results mean value. Standard deviations of the real and imaginary parts of each measured voltage is on the level of 0,1 µV.

4.4. Measurement procedure

Measurement procedure connected with the unbalanced comparator is described in few following steps:

1. The values of the DSS settings $\underline{K'_{IJ}}$, $\underline{K''_{IJ}}$ are determined from (7-8). The variable $\underline{K_P}$ may be equal to 1.
2. The voltage ratios $\underline{K'_{IJV}}$, $\underline{K''_{IJV}}$ and values of the relative unbalance voltages $\underline{U'_{D,r}}$, $\underline{U''_{D,r}}$ are measured.
3. The impedance ratio $\underline{K_Z}$ is determined using (4) and the more accurate value of $\underline{K_P}$ is derived from

$$\underline{K_P} = -0.5\left(\frac{\underline{k'_r}+1}{\underline{K_Z}} + \frac{\underline{k''_r}+1}{\underline{K_Z}}\right),$$

where:

$$\underline{k'_r} = \frac{\underline{K_Z}-\underline{K'_{IJV}}}{\underline{U'_{D,r}}},\ \underline{k''_r} = \frac{\underline{K_Z}-\underline{K''_{IJV}}}{\underline{U''_{D,r}}}.$$

4. New values of the settings $\underline{K'_{IJ}}$, $\underline{K''_{IJ}}$ are computed using a new value of $\underline{K_P}$.
5. After the values of $\underline{U'_{D,r}}$, $\underline{U''_{D,r}}$, $\underline{K'_{IJV}}$, $\underline{K''_{IJV}}$ are measured the final value of $\underline{K_Z}$ is determined from (4).

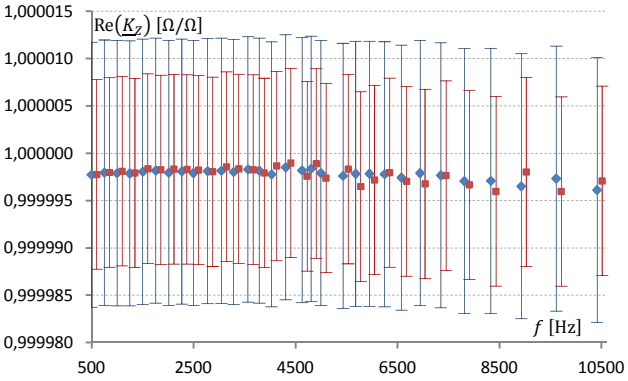

Fig. 6. The real part of the R-R comparison (10 kΩ – 10 kΩ).

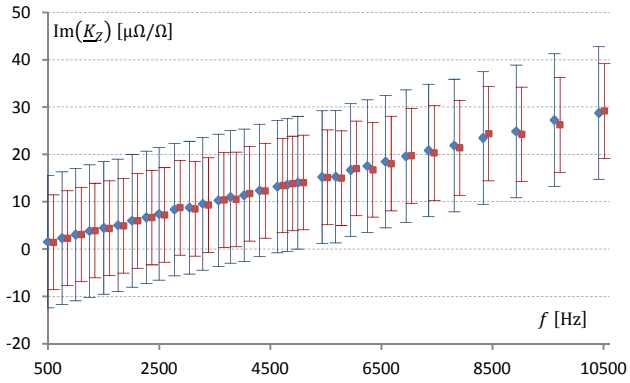

Fig. 7. The imaginary part of the R-R comparison (10 kΩ – 10 kΩ).

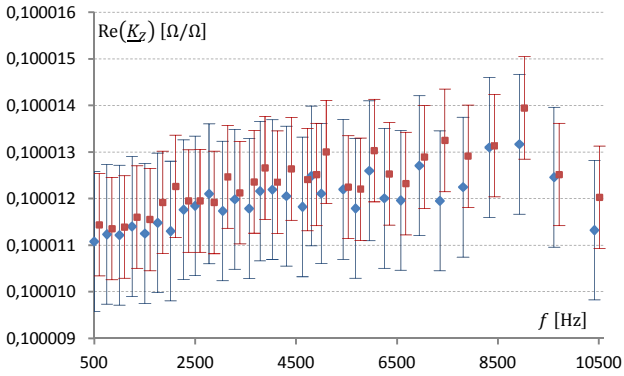

Fig. 8. The real part of the R-R comparison (10 kΩ – 100 kΩ).

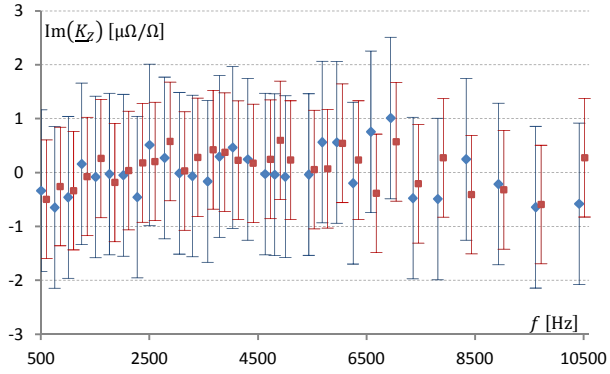

Fig. 9. The imaginary part of the R-R comparison (10 kΩ – 100 kΩ) (regression).

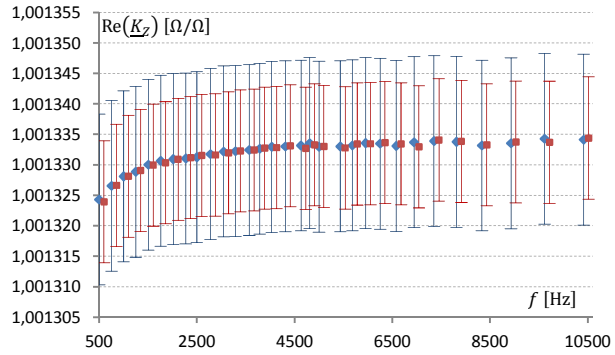

Fig. 10. The real part of the C-C comparison (3 nF – 3 nF).

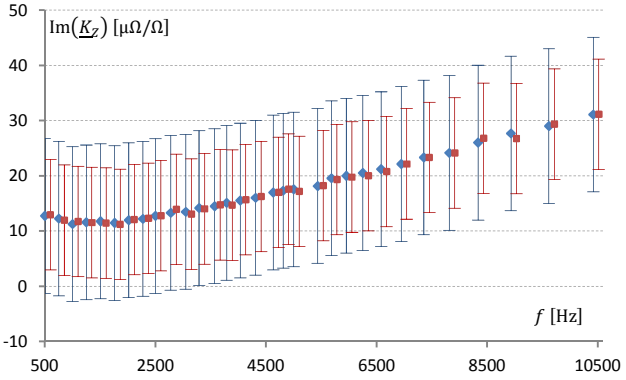

Fig. 11. The imaginary part of the C-C comparison (3 nF – 3 nF).

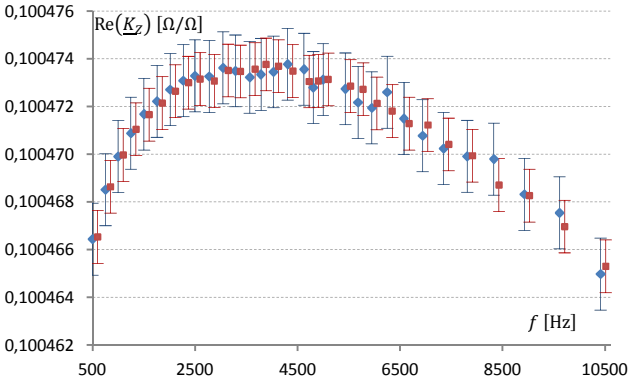

Fig. 12. The real part of the C-C comparison (10 nF – 1 nF).

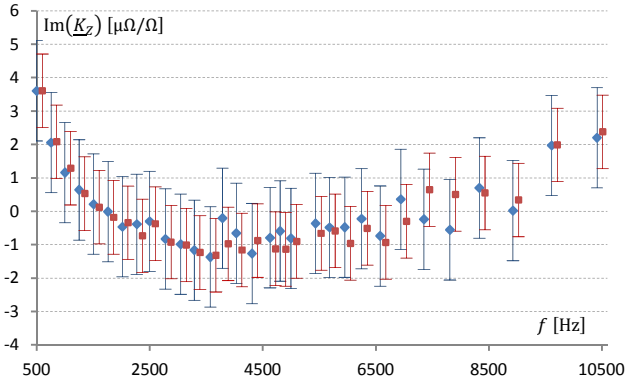

Fig. 13. The imaginary part of the C-C comparison (10 nF – 1 nF) (regression).

4.5. Conclusions

The experimental results shown in Fig. 6-13 do not differ more than the evaluated measurement errors. The higher spread of the results can be observed for the comparison of the impedances which have 1:10 modulus ratio. This may be caused by the linearity errors which may have higher values for lower voltages than it is assumed in (19).

The time required to measure the impedance ratio by the unbalanced comparators is approximately equal to 45 seconds. The time required to measure the impedance ratio by the balanced comparator is varying. When the resolution of the DSS settings is deteriorating the balance process is getting longer. The time needed by the unbalanced comparator to measure the impedance ratio is always the same and it does not depend on the frequency or the values of the compared impedances.

Regression was used to make the values and errors in Fig. 9 and Fig. 13 more readable.

5. SUMMARY

The theoretical studies and the experimental results shown in this article prove that the digital unbalanced comparator with interpolation is able to measure the impedance ratio with the same accuracy as the digital balanced comparator do. For higher frequencies or for lower resolution of the DSS settings the bridge cannot be balanced and we have to use the unbalance voltage to measure the impedance ratio.

The time required to take a measurement by the unbalanced comparator is generally shorter than corresponding time required in the balanced comparator. More researches are needed to determine how the time of the measurement affects the accuracy of the presented digital unbalanced comparator.

Equation describing the measurement system is accurate to approximately 10 kHz. Above that frequency more extended model should be used.

The author wish to employ the digital unbalanced comparator for 4TP impedance measurements.

REFERENCES

[1] Helbach W., Marczinowski P., Trenkler G., “High-Precision Automatic Digital AC Bridge”, *IEEE Trans. on Instr. and Meas.*, vol. IM-32, nº. 1, pp. 159-162, 1983.

[2] Helbach W., Shollmeyer H., “Impedance Measuring Methods Based on Multiple Digital Generators”, *IEEE Trans. on Instr. and Meas.*, vol. IM-36, nº. 2, pp. 400-405, 1987.

[3] Waltrip B. C., Oldham N. M., “Digital Impedance Bridge”, *IEEE Trans. on Instr. and Meas.*, vol. 44, nº. 2, pp. 436-439, 1995.

[4] Betta G., Liguori C., Pietrosanto A., “Propagation of uncertainty in a discrete Fourier transform algorithm”, *Measurement*, vol. 27, nº. 4, pp. 231-239, June 2000.

[5] Ramm G., Moser H., “New Multifrequency Method for the Determination of the Dissipation Factor of Capacitors and of the Time Constant of Resistors”, *IEEE Trans. on Instr. and Meas.*, vol. 54, nº. 2, pp. 521-524, 2005.

[6] Rybski R., Kaczmarek J., Kontorski K.: „Impedance Comparison Using Unbalance Bridge with Digital Sinevawe Sources”, *IEEE Trans. on Instr. and Meas.*(*IEEE Early Access Articles*), vol. PP, nº. 99, 2015.